# Relative and Absolute Configurational Assignments of Acyclic Polyols by Circular Dichroism. 2.[1] Determination of Nondegenerate Exciton Coupling Interactions by Assignment of Prochiral Aryloxymethylene Protons for $^1$H NMR Conformational Analysis

**William T. Wiesler[†] and Koji Nakanishi***

*Contribution from the Department of Chemistry, Columbia University, New York, New York 10027.* *Received October 18, 1989*

**Abstract:** A general procedure for assigning relative and absolute stereochemistry in 1,2,3-triols, 1,2,3,4-tetrols, and 1,2,3,4,5-pentols by circular dichroism was recently reported. Selective 9-anthroylation of primary hydroxyls followed by per-*p*-methoxycinnamoylation of secondary hydroxyls affords "bichromophoric" derivatives, the CD spectra of which are *characteristic and predictable for each stereochemical pattern.* The distinctive CD spectra result from two types of exciton coupling interactions: degenerate cinnamate/cinnamate interactions that give rise to Cotton effects at 287 and 322 nm, and nondegenerate anthroate/cinnamate interactions that result in a strong sharp Cotton effect at 253 nm and smaller Cotton effects in the 300–380-cm region. The 287- and 322-nm Cotton effects were previously accounted for by consideration of the additive contributions from pairwise cinnamate/cinnamate interactions in $^1$H NMR determined conformations. Here the 253-nm Cotton effects are accounted for by analysis of the anthroate/cinnamate exciton coupling modes. These have been determined by NMR, for which stereospecifically deuterated compounds **1** and **2** were prepared from (6*S*)-(6-$^2H_1$)-1-deoxy-D-galactitol and (6*S*)-(6-$^2H_1$)-1-deoxy-D-glucitol, respectively, in order to assign *pro-R* and *pro-S* protons in anthroyloxymethylene groups. Distributions of the three staggered anthroyloxymethyl rotamers were calculated from vicinal coupling constants. CD spectral contributions of anthroate/cinnamate interactions in the dominant rotamers were determined via model compounds and shown to account for the predominance of positive 253-nm Cotton effects in these derivatives. The large number of acyclic derivatives allowed for graphical analysis of the interdependence between C1–C2 and C2–C3 rotamers for conformational analysis. Exciton coupling interactions between 1-*O*-(9-anthroate) and 3-*O*-*p*-methoxycinnamate groups have been elucidated for both 2,3-erythro and threo configurations, and in certain cases minor conformations were found to be responsible for distinctive features of the CD spectra.

The exciton chirality method has been widely used for assigning absolute configuration in natural products by circular dichroism (CD).[2] The method is most commonly applied to compounds bearing one or more hydroxyl groups that may be derivatized with an exciton-coupling chromophore such as the *p*-bromobenzoate ester. A recent extension of this method utilizes two types of exciton chromophores simultaneously that have been selectively introduced to two different types of hydroxyl groups.[3] This technique constitutes the basis of an oligosaccharide microanalysis,[4] in which free hydroxyls are converted to bromobenzoates, and then, following cleavage of the glycosidic linkages, the liberated hydroxyls are tagged with the red-shifted methoxycinnamate groups. CD spectra of the resulting components indicate the types of sugars and their linkage patterns at nanomole levels. These characteristic CD curves result from the additive effects of all pairwise interchromophoric interactions and therefore can be accurately simulated by spectral summation of pairwise contributions.[4]

We recently reported that relative and absolute stereochemistry in acyclic 1,2,3-triols can be easily determined by a similar CD technique that utilizes two types of chromophores.[5] For this application, the strongly absorbing 9-anthroate chromophore was chosen because it can be selectively introduced to primary hydroxyls.[6] Subsequent per-*p*-methoxycinnamoylation of secondary hydroxyls affords "bichromophoric" derivatives, the CD spectra of which are characteristic for each stereochemical pattern. Similarly, we have found that this CD method can be used to assign the three chiral centers in acyclic 1,2,3,4-tetrols and even four chiral centers in acyclic 1,2,3,4,5-pentols.[1] While this simple yet powerful method can be used empirically, we have demonstrated the predictable nature of the resulting CD curves for different stereochemical patterns.[1]

In the acyclic polyol derivatives bearing an anthroate and two or more methoxycinnamate ester groups, there are two different types of pairwise exciton-coupling interactions between chromophores:

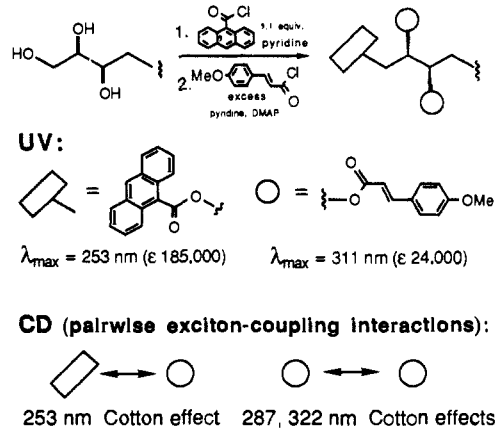


Anthroate/methoxycinnamate interactions give rise to very strong,

[†] Present address: Department of Chemistry and Biochemistry, University of Colorado, Boulder, Colorado 80309.

(1) Part 1: Wiesler, W. T.; Nakanishi, K. *J. Am. Chem. Soc.* **1989**, *111*, 9205-9213.

(2) Harada, N.; Nakanishi, K. *Circular Dichroic Spectroscopy-Exciton Coupling in Organic Stereochemistry*; University Science Books: Mill Valley, CA, 1983.

(3) Wiesler, W. T. Pairwise Additivity in Circular Dichroism: Applications to Oligosaccharide and Acyclic Polyol Structural Analysis. Ph.D. Dissertation, 1989, Columbia University, New York, NY 10027.

(4) (a) Wiesler, W. T.; Vāzquez, J. T.; Nakanishi, K. *J. Am. Chem. Soc.* **1987**, *109*, 5586-5592. (b) Vāzquez, J. T.; Wiesler, W. T.; Nakanishi, K. *Carbohydr. Res.* **1988**, *176*, 175. (c) Meyers, H. V.; Ojika, M.; Wiesler, W. T.; Nakanishi, K. *Carbohydr. Res.* **1990**, *197*, 15-32. (d) Ojika, M.; Meyers, H. V.; Chang, M.; Nakanishi, K. *J. Am. Chem. Soc.* **1989**, *111*, 8944-8946.

(5) Wiesler, W. T.; Nakanishi, K. *J. Am. Chem. Soc.* **1989**, *111*, 3446-3447.

(6) Wiesler, W. T.; Nakanishi, K. *Croat. Chim. Acta* **1989**, *62*, 211-226.

0002-7863/90/1512-5574$02.50/0 

**Table I.** $^1$H NMR Data for C2–C3 Erythro Derivatives: Assignments of Prochiral Protons at C1 Based upon Chirally Deuterated Derivative **2**; Calculated Populations of C1–C2 Rotamers; and Additional Conformation-Dependent NMR and CD Data[a]

| class | no.[b] | H1S | $J_{1S-2}$ | H1R | $J_{1R-2}$ | $P_{gg}$ | $P_{gt}$ | $P_{tg}$ | $J_{2-3}$ | $H_\alpha$[c] | 253 nm[d] |
|---|---|---|---|---|---|---|---|---|---|---|---|
| erythro | **8a** | 4.95 | 3.7 | 4.87 | 6.4 | 0.41 | 0.42 | 0.17 | 4.6 | 6.32 | +31 |
| | **8b** | 4.95 | 3.6 | 4.88 | 6.5 | 0.40 | 0.44 | 0.16 | 4.6 | 6.34 | +45 |
| | **8c** | 4.90 | 5.1 | 4.90 | 5.1 | | | | 4.6 | 6.36 | +42 |
| | **8d** | 5.10 | 3.0 | 4.84 | 5.2 | 0.56 | 0.32 | 0.12 | 6.5 | 6.33 | +34 |
| ribo | **13a** | 5.08 | 2.8 | 4.86 | 6.3 | 0.46 | 0.46 | 0.08 | 6.0 | 6.33 | +52 |
| | **13b** | 5.12 | 2.8 | 4.87 | 6.5 | 0.45 | 0.47 | 0.08 | 5.5 | 6.33 | +41 |
| | **13c** | 5.12 | 2.7 | 4.85 | 5.5 | 0.54 | 0.38 | 0.08 | 6.0 | 6.35 | +39 |
| | **13d** | 5.10 | 2.6 | 4.93 | 6.9 | 0.42 | 0.53 | 0.05 | 4.4 | 6.32 | +47 |
| arabino | **14a** | 5.03 | 2.9 | 4.81 | 5.6 | 0.52 | 0.38 | 0.10 | 7.1 | 6.33 | +26 |
| | **14b**[e] | 5.02 | 2.8 | 4.80 | 5.3 | 0.55 | 0.35 | 0.10 | 6.7 | 6.35 | +18 |
| | **14c** | 5.04 | 2.8 | 4.82 | 5.2 | 0.56 | 0.34 | 0.10 | 7.1 | 6.34 | +20 |
| | **14d** | 4.99 | 3.6 | 4.80 | 5.9 | 0.45 | 0.38 | 0.17 | 6.0 | 6.32 | +38 |
| allo | **17** | 5.14 | 2.8 | 4.97 | 6.4 | 0.46 | 0.46 | 0.08 | 4.9 | 6.26 | +42 |
| altro | **18** | 5.13 | 2.7 | 4.92 | 6.3 | 0.47 | 0.46 | 0.07 | 4.9 | 6.26 | +39 |
| gluco | **19**[e] | 5.03 | 3.2 | 4.84 | 5.7 | 0.50 | 0.37 | 0.13 | 6.4 | 6.20 | +22 |
| manno | **20** | 5.07 | 3.2 | 4.82 | 5.4 | 0.51 | 0.35 | 0.14 | 6.9 | 6.12 | +23 |
| glycero | **9** | 4.87 | 3.5 | 4.70 | 6.4 | 0.42 | 0.43 | 0.15 | | 6.36 | +28 |

[a] Chemical shifts are reported in ppm. First-order coupling constants are reported in Hz. [b] Compound numbers from ref 1, in which alkyl substitution is represented as follows: **a**, Me; **b**, Et; **c**, CH=CH$_2$; and **d**, CH(SEt)$_2$. [c] Chemical shift of the methoxycinnamate vinylic proton $\alpha$ to the carbonyl which appears furthest upfield. [d] $\Delta\epsilon$ of Cotton effect in CD. [e] Deuterated compounds prepared.

sharp Cotton effects (CEs) in CD spectra at 253 nm, the absorption maximum of the anthroate chromophore, in addition to smaller CEs around 311 nm (cinnamate absorption maximum) and 350–380 nm (minor anthroate transitions). Cinnamate/cinnamate interactions give rise to CEs of opposite sign at 287 and 322 nm. By $^1$H NMR conformational analysis, the signs and magnitudes of the 287/322-nm CEs in all of the acyclic polyol derivatives were accounted for by considering the pairwise cinnamate/cinnamate interactions in both major and minor conformations.[1]

We report herein that the signs and magnitudes of the 253-nm Cotton effects resulting from anthroate/cinnamate interactions can also be accounted for in the acyclic polyol derivatives. For $^1$H NMR conformational analysis, the prochiral protons of the anthroyloxymethylene groups have been assigned by stereospecific deuteration, and rotameric distributions at this position have been calculated. The various anthroate/cinnamate coupling modes associated with predominant conformations have been elucidated. In certain cases, we show that a minor, folded conformation in which aromatic groups are stacked can contribute to dramatic changes in the intensity and sometimes the sign of the 253-nm Cotton effect. The ability to account for the signs and intensities of Cotton effects that characterize each stereochemical pattern in acyclic polyol derivatives reflects the nonempirical basis of the exciton chirality method for stereochemical studies.

## Results and Discussion

**Assignment of Prochiral Hydroxymethyl Protons.** In order to assign the prochiral protons at C1[7] in the previously reported series of acyclic polyol derivatives, the corresponding chirally deuterated derivatives **1** and **2** were prepared:

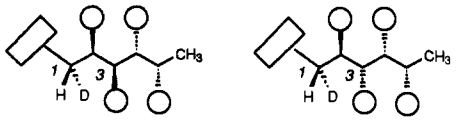


**1** **2**

These two C3 epimers were chosen as representative examples to determine whether the configuration at this position would affect the assignment of the protons at C1. Chiral deuterations were carried out by using the excellent procedures developed by Ohrui and co-workers.[8] For example, (6*S*)-(6-deuterio)-D-galactose **4** was prepared in six steps[8a] from 1,6-anhydro-D-galactopyranose **3** in 18% overall yield:

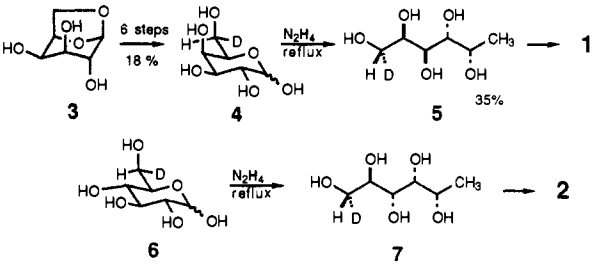


This was converted to (6*S*)-(6-deuterio)-1-deoxy-D-galactitol **5** by using the hydrazinolysis conditions of Williams,[9] which we had previously applied to all of the D-aldose sugars to prepare a series of acyclic polyols.[5] The deuterated galactitol **5** was derivatized in the usual fashion[1,5] depicted above with 1.1 equiv of 9-anthroyl chloride,[10] followed by treatment of the monoester intermediate with excess *p*-methoxycinnamoyl chloride[11] to afford **1**. Likewise, (6*S*)-(6-deuterio)-D-glucose[7b] was converted to the chirally deuterated derivative **2**.

The partial $^1$H NMR spectra of **1** and the corresponding undeuterated derivative **24**[12] are shown in Figure 1. The 5.06-ppm dd in **24** is reduced to 5% of its original intensity[13] upon deuteration of the *pro-S* position, while the 4.75-ppm dd assigned to H1R in **24** collapses to a doublet in **1**[14] and the 5.7 multiplet assigned to H2 becomes a clear doublet of doublets. Similarly, comparison of **2** to its corresponding undeuterated analogue (**19**) indicated again that the H1S proton is downfield of H1R. The assignments

(7) For continuity in comparing NMR data of the various triol, tetrol, and pentol derivatives, and for relevance to natural products, the position of the primary hydroxyl has been designated C-1. (By conventional carbohydrate nomenclature, this is C-4 in tetrose derivatives, C-5 in pentose derivatives, and C-6 in hexose derivatives).

(8) (a) Ohrui, H.; Nishida, Y.; Meguro, H. *Agric. Biol. Chem.* **1984**, *48*, 1049–1053. (b) Ohrui, H.; Horiki, H.; Kishi, H.; Meguro, H. *Agric. Biol. Chem.* **1983**, *47*, 1101–1106.

(9) Williams, J. M. *Carbohydr. Res.* **1984**, *128*, 73.

(10) Prepared from the acid (1 g) and either oxalyl chloride (2 mL) or thionyl chloride (4.5 mL) in refluxing dry benzene (1 h). Benzene and excess reagent were removed in vacuo to afford 9-anthracenecarbonyl chloride as a yellow solid.

(11) Prepared from the acid and thionyl chloride (1.2 equiv) in refluxing benzene (2 h). Benzene and excess reagent were removed in vacuo, and distillation in a sublimation apparatus (140 °C (0.1 mmHg)) afforded the pure acid chloride.

(12) For the sake of consistency between this paper and Part 1 (ref 1), numbers designating compounds **8** through **24** used in Part I are repeated here.

(13) Deuteration is carried out with tri-*n*-butyltin deuteride (Alfa), which has a deuterium content of ~95%.

(14) This H1R signal was shifted slightly upfield as a result of the deuterium isotope effect.

**Table II.** $^1$H NMR Data for C2–C3 Threo Derivatives: Assignments of Prochiral Protons at C1 Based upon Chirally Deuterated Derivative **1**; Calculated Populations of C1–C2 Rotamers; and Additional Conformation-Dependent NMR and CD Data[a]

| class | no.[b] | H1S | $J_{1S-2}$ | H1R | $J_{1R-2}$ | $P_{gg}$ | $P_{gt}$ | $P_{tg}$ | $J_{2-3}$ | $H_\alpha$[c] | 253 nm[d] |
|---|---|---|---|---|---|---|---|---|---|---|---|
| threo[e] | **11a** | 4.93 | 3.3 | 4.75 | 6.6 | 0.41 | 0.46 | 0.13 | 4.5 | 6.26 | +24 |
| | **11b** | 4.96 | 3.3 | 4.77 | 6.6 | 0.41 | 0.46 | 0.13 | 5.7 | 6.30 | +17 |
| | **11c** | 5.12 | 3.7 | 4.71 | 4.6 | 0.56 | 0.24 | 0.20 | 5.6 | 6.14 | +8 |
| xylo[f] | **15a** | 5.00 | 3.4 | 4.71 | 6.0 | 0.45 | 0.40 | 0.15 | 4.7 | 6.20 | +23 |
| | **15b** | 5.04 | 3.2 | 4.74 | 5.6 | 0.51 | 0.36 | 0.13 | 5.3 | 6.18 | +24 |
| | **15c** | 5.03 | 3.6 | 4.71 | 5.6 | 0.48 | 0.34 | 0.18 | 4.7 | 6.12 | +17 |
| | **15d** | 5.00 | 3.7 | 4.74 | 5.9 | 0.45 | 0.37 | 0.18 | 3.9 | 6.17 | +21 |
| lyxo[f] | **16a** | 4.98 | 3.7 | 4.77 | 6.4 | 0.40 | 0.43 | 0.17 | 3.6 | 6.19 | +7 |
| | **16b** | 4.97 | 4.0 | 4.74 | 6.3 | 0.40 | 0.40 | 0.20 | 3.2 | 6.14 | -6 |
| | **16c** | 4.99 | 3.7 | 4.76 | 6.2 | 0.42 | 0.40 | 0.18 | 3.4 | 6.16 | -1 |
| | **16d** | 5.02 | 4.3 | 4.75 | 6.3 | 0.38 | 0.38 | 0.24 | 1.8 | 6.12 | 0 |
| gulo | **21** | 5.05 | 3.4 | 4.78 | 5.0 | 0.55 | 0.29 | 0.16 | 5.3 | 6.02 | +10 |
| ido | **22** | 5.06 | 3.8 | 4.76 | 5.3 | 0.50 | 0.30 | 0.20 | 4.7 | 6.13 | +10 |
| galacto | **23**[g] | 5.05 | 4.3 | 4.68 | 5.5 | 0.45 | 0.30 | 0.25 | 2.3 | 6.00 | -5 |
| talo | **24** | 5.06 | 4.2 | 4.75 | 5.9 | 0.42 | 0.35 | 0.23 | 2.9 | 6.12 | -7 |

[a] Chemical shifts are reported in ppm. First-order coupling constants are reported in Hz. [b] Compound numbers from ref 1. [c] Chemical shift of the methoxycinnamate vinylic proton $\alpha$ to the carbonyl which appears furthest upfield. [d] $\Delta\epsilon$ of Cotton effect in CD. [e] Alkyl substitution is represented as follows: **a**, Et; **b**, CH=CH$_2$; and **c**, CH(SEt)$_2$. [f] Alkyl substitution is represented as follows: **a**, Me; **b**, Et; **c**, CH=CH$_2$; and **d**, CH(SEt)$_2$. [g] Deuterated compound prepared.

made for these derivatives can be easily extended to the entire, previously reported series of acyclic polyols, which can be divided into two groups:

2,3 Erythro (Table I):

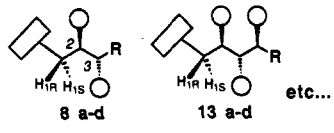


2,3 Threo (Table II):

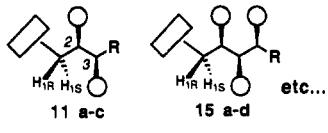


Assignments of H1S and H1R for derivatives with erythro stereochemistry between C2 and C3 based upon comparison with **2** are listed in Table I. Similarly, assignments of H1S and H1R for derivatives with threo stereochemistry between C2 and C3 based upon comparison with **1** are listed in Table II.

**Rotameric Distributions about C1–C2 Bonds.** Newman projections of the three possible staggered conformations about the C1–C2 bond are shown in Figure 2. The conventional designations **gg**, **gt**, and **tg** have been ascribed to them, wherein the first letter indicates the relative orientation between O1 and O2 (gauche or trans) while the second letter indicates the orientation between O1 and the alkyl group R. It is generally assumed that these staggered rotamers represent minimum free energy conformations. We can also assume that the observed vicinal spin–spin coupling constants represent weighted averages of the component coupling constants associated with each of the three rotamers.

The $J_{1S-2}$ coupling constants listed in Table I and II are consistently small (2.6–4.3 Hz), indicative of a predominantly gauche orientation between these two protons. The $J_{1R-2}$ coupling constants are always larger (5.1–6.9 Hz), and such intermediate values (i.e. between ~2 Hz for gauche and ~10 Hz for anti) indicate that the relative orientation between H1R and H2 equilibrates between gauche and anti. Inspection of Figure 2 reveals that a mixture of **gg** and **gt** rotamers best explains this NMR data, and therefore these two rotamers must predominate. Such a preference for conformations in which the oxygen atoms adopt gauche orientations can be ascribed to the well-known "gauche effect".

The distribution of rotamers can be determined more quantitatively by using equations that describe the observed coupling constants as averages of the component coupling constants for the three rotamers weighted by the mole fraction of each. Distributions of C4–C5 rotamers in pentofuranosides[15,16] and C5–C6 rotamers in hexopyranosides,[4a,17] including (1–6)-linked di-

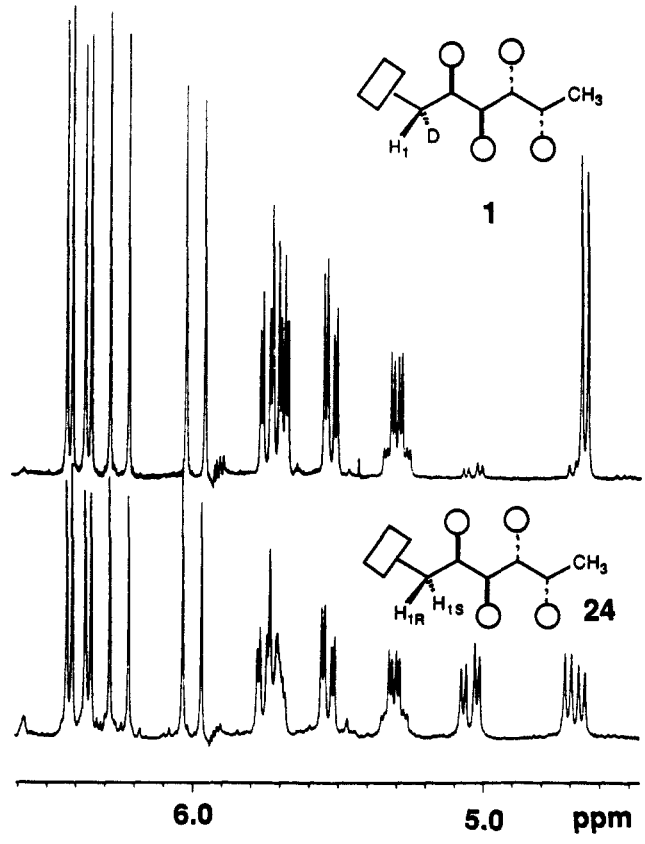


**Figure 1.** NMR assignment of prochiral aryloxymethylene protons by chiral deuteration. Partial $^1$H NMR spectrum of (6*S*)-(6-$^2$H$_1$)-1-deoxy-D-galactitol 6-(9-anthroate) 2,3,4,5-tetra-*p*-methoxycinnamate superimposed with undeuterated compound indicating the position of the *pro-S* proton at 5.05 ppm. Also shown are the four vinylic protons (6.0–6.4 ppm) belonging to the cinnamate groups, of which one is significantly shifted upfield from the others. This upfield shift is characteristic of derivatives having threo configuration between the two asymmetric centers proximal to the anthroate group.

(15) Gerlt, J. A.; Youngblood, V. *J. Am. Chem. Soc.* **1980**, *102*, 7433–7438.
(16) Wu, G. D.; Serianni, A. S.; Barker, B. *J. Org. Chem.* **1983**, *48*, 1750–1757.
(17) (a) Nishida, Y.; Ohrui, H.; Meguro, H. *Tetrahedron Lett.* **1984**, *25*, 1575–1578. (b) Ohrui, H.; Nishida, Y.; Higuchi, H.; Hori, H.; Meguro, H. *Can. J. Chem.* **1987**, *65*, 1145–1153. (c) Nishida, Y.; Hori, H.; Ohrui, H.; Meguro, H. *J. Carbohydr. Chem.* **1988**, *7*, 239–250.

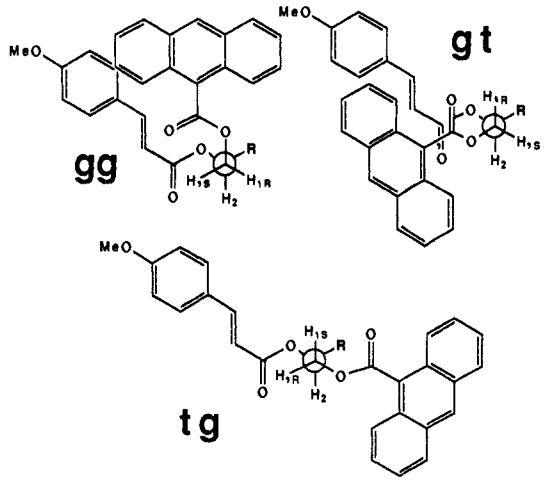


**Figure 2.** Newman projections of the three possible rotamers about the C1–C2 bond.

saccharides,[18] have been calculated by using the following equations:

$$1.3P_{gg} + 2.7P_{gt} + 11.7P_{tg} = J_{1S\text{-}2}$$

$$1.3P_{gg} + 11.5P_{gt} + 5.8P_{tg} = J_{1R\text{-}2}$$

$$P_{gg} + P_{gt} + P_{tg} = 1$$

There are uncertainties in the precise mole fractions (i.e. $P_{gg}$, etc.) obtained from such equations owing to uncertain coupling constant values for each rotamer (generally determined via Karplus type equations), deviations of dihedral angles from the assumed 60° or 180°, and other factors. However, such uncertainties are inconsequential to this study as we are interested in using calculated distributions of C1–C2 rotamers only to indicate general trends in the distribution of these rotamers.

Mole fractions of the three C1–C2 rotamers for each of the 32 acyclic polyol derivatives have been calculated with the above equations and are listed in Tables I and II. As expected, the calculations indicate that **gg** and **gt** are the major rotamers in all cases. The proportion of the **tg** rotamer, which is associated with a large $J_{1S\text{-}2}$, is somewhat greater in the C2–C3 threo derivatives (13–25%, Table II) than in erythro derivatives (5–17%, Table I). This reflects the larger $J_{1S\text{-}2}$ values in threo vs erythro cases (average $J_{1S\text{-}2}$'s: 3.7 Hz vs 3.1 Hz, respectively). Thus, the configuration at C3 clearly affects the distribution of C1–C2 rotamers, as indicated by the erythro/threo differences. In fact, examination of the tabulated distributions reveals that even the configuration at C4 affects C1–C2 rotamers, as illustrated by the differences between ribo and arabino derivatives (Table I). The configuration of the fourth asymmetric center at C5, however, does not influence the distribution of C1–C2 rotamers, as seen by the similarities between allo (**17**) and altro (**18**) or again between gluco (**19**) and manno (**20**) derivatives (Table I).

**Anthroate/C2-Cinnamate Interactions Contributing to CD.** Having determined the distribution of the C1–C2 rotamers that are depicted in Figure 2, we sought to assess the contributions of anthroate/C2-cinnamate exciton-coupling interactions within each rotamer to the CD spectra of the acyclic polyol derivatives. The possible contribution of anthroate/C2-cinnamate coupling in rotamer **tg** was considered negligible, not only because of the small percentage of this rotamer which exists but also because of the large interchromophoric distance that occurs in this rotamer between anthroate and cinnamate groups (see Figure 2). (The intensity of Cotton effects resulting from exciton coupling is proportional to $1/R^2$, where $R$ is the distance between the center of coupling transitions.[2]) Thus, the major rotamers **gg** and **gt** are expected to make the most significant contributions to CD spectra.

(18) (a) Nishida, Y.; Hori, H.; Ohrui, H.; Meguro, H.; Uzawa, J. *Tetrahedron Lett.* **1988**, *29*, 4461–4464. (b) Hori, H.; Nishida, Y.; Ohrui, H.; Meguro, H.; Uzawa, J. *Tetrahedron Lett.* **1988**, *29*, 4457–4460.

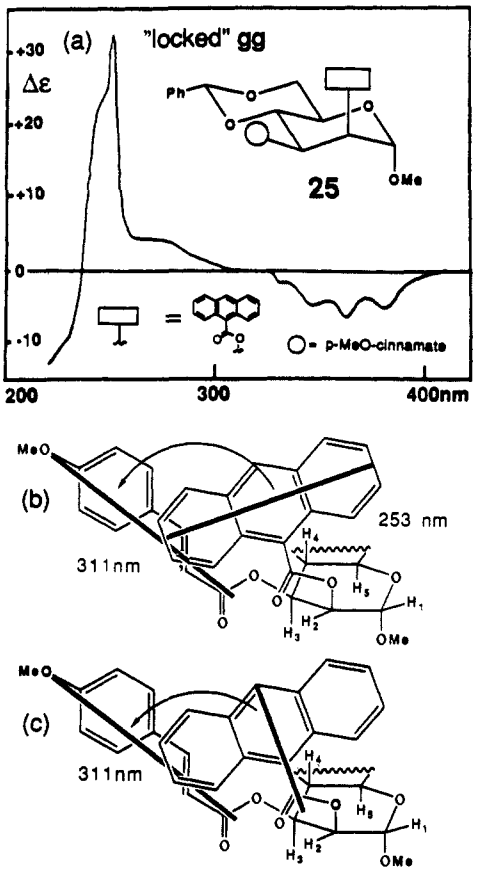


**Figure 3.** (a) CD spectrum of a "locked" **gg** model compound, representing the contribution which anthroate/C2-cinnamate coupling in the **gg** rotamer would make to CD curves of acylic polyol derivatives. (b) Negative chirality depicted between the long axis anthroate transition at 253 nm and the cinnamate transition at 311 nm. The chirality is shown to be negative by the counterclockwise rotation between the two transitions and thus is predicted to give rise to a negative first CE at 311 nm and a positive second CE at 253 nm in the CD spectrum. (c) Negative chirality depicted between the short axis anthroate transitions in the 350–380-nm region and the cinnamate transition at 311 nm. Exciton coupling between these is expected to give rise to negative first CEs around 350–380 nm and a positive second CE at 311 nm in the CD spectrum. The latter effect at 311 nm and the opposite effect at this position from coupling shown in (b) cancel out.

The CD contributions of each major rotamer can be determined by means of model compounds in which the anthroate and cinnamate chromophores are rigidly fixed with the appropriate orientations. This has been achieved by derivatization of manno- and glucopyranoside 4,6-benzylidene acetals with the 9-anthroate and methoxycinnamate esters at the 2- and 3-positions. The bicyclic ring sugars were used to maintain the desired chair conformation, ensuring a typical staggered conformation between the vicinal chromophoric groups. Placement of the anthroate at the 2-position and cinnamate at the 3-position results in identical absolute stereochemistry between the two chromophores as in the series of acyclic polyols above.

The CD curve of the "locked" **gg** model derived from methyl mannopyranoside is shown in Figure 3. The spectrum is characterized by a strong positive 253-nm CE, which results from exciton coupling of the long axis anthroate transition with the cinnamate transition. As shown in Figure 3b, the counterclockwise orientation between the two transitions indicates a negative chirality. This means that the resulting couplet in the CD spectrum can be expected to exhibit a negative first CE (long wavelength) and a positive second CE (short wavelength). While the second CE at 253 nm is readily apparent, a first CE at 311 nm is not observed. This is due to superimposition of an additional couplet resulting from coupling of the cinnamate with the short axis transitions of the anthroate chromophore which absorb at higher wavelengths. As depicted in Figure 3c, a negative chirality

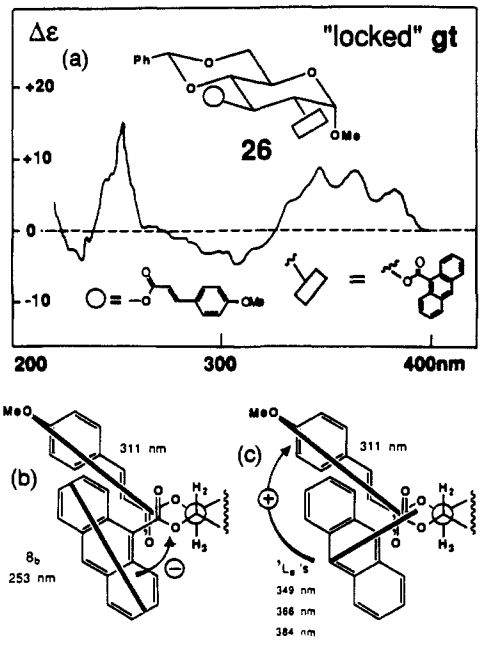


Figure 4. (a) CD spectrum of a "locked" gt model compound, representing the contribution of anthroate/C2-cinnamate coupling in the gt rotamer. (b) Negative chirality between the long axis anthroate transition at 253 nm and the cinnamate transition at 311 nm, which results in the negative CE at 311 nm and the positive CE at 253 nm. (c) Positive chirality between the short axis anthroate transitions (350–380 nm) and the cinnamate transition (311 nm) responsible for the positive CEs around 350–380 nm and contributing to the negative CE at 311 nm.

is expected for this coupling as well. This gives rise to the negative first CEs observed in the 350–380-nm regions and results in the cancelling of effects at 311 nm.

The CD curve of the analogous "locked" gt model derived from methyl glucopyranoside is shown in Figure 4. A positive yet smaller 253-nm CE is also observed for this derivative, in addition to a negative CE at 311 nm and surprisingly strong CEs in the 350–380-nm region. Again, negative chirality between the long axis anthroate and cinnamate transitions is observed, only here the dihedral angle between them is rather small (<30°). Coupling intensity is strongly dependent upon this dihedral angle $\theta$: calculations have shown it to be maximal when $\theta \sim 70°$ and zero when $q = 0°$ or 180°.[1,19] This explains why the 253-nm CE in **26** (Figure 4) is so much smaller than the same CE in **25** (Figure 3). This same dependence upon dihedral angle between transitions accounts for the rather large CEs in the 350–380-nm range. As shown in Figure 4c, these transitions couple with the cinnamate giving rise to a positive chirality (clockwise, hence the positive first CEs at long wavelength), and the dihedral angle between the two is nearly optimal (i.e., ~70°). While the extinction coefficients of the long and short axis anthroate transitions vary greatly ($\epsilon$ 185 000 vs $\epsilon \sim 10\,000$, respectively), and considering that the intensity of exciton coupling is proportional to $\epsilon^2$,[20] it is interesting to see the two transitions giving rise to CEs of nearly the same size. The CD curve of **26** is an excellent illustration of the dependence of exciton coupling upon dihedral angle. The negative CE around 310 nm arises from overlap of two negative CEs: the first CE associated with the interaction depicted in Figure 4b, and the second CE resulting from the interaction shown in Figure 4c.

Having modeled the CD contributions of the major C1–C2 rotamers, we can see that the positive 253-nm CEs of each undoubtedly contribute to the preponderance of positive 253-nm CEs among the series of acyclic polyol derivatives (Tables I and II). The simplest case among these with only a single asymmetric center is the (*S*)-1,2-propanediol 1-*O*-(9-anthroate) 2-*O*-methoxycinnamate derivative **9**, for which an equal proportion of **gg** and **gt** rotamers is predicted (Table I). The CD spectrum of **9** is shown in Figure 5 together with the averaged CD of the "locked" **gg** and **gt** derivatives. This "calculated" spectrum simulates the sign and intensity of the 253-nm CE as well as the somewhat featureless 280–380-nm region of the spectrum of **9** rather well. Thus, exciton-coupling interactions between the anthroate and C2-methoxycinnamate chromophores, which occur in the major **gg** and **gt** C1–C2 rotamers, clearly account for the characteristic positive 253-nm CE present in the CD curves of nearly all of the above polyol derivatives.

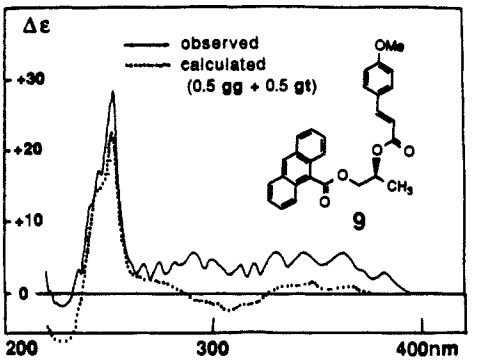


Figure 5. CD spectrum of (*S*)-1,2-propanediol 1-*O*-(9-anthroate) 2-*O*-methoxycinnamate derivative **9**, for which an equal proportion of **gg** and **gt** rotamers is predicted. The averaged CD of the "locked" **gg** and **gt** derivatives is shown to simulate the observed spectrum well, confirming that exciton coupling in these two rotamers accounts for the CD spectrum of **9**.

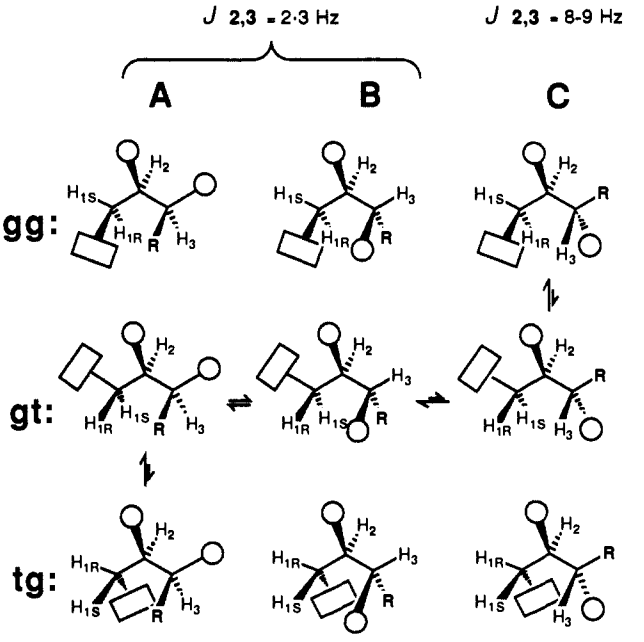


Figure 6. The nine possible conformations of C1–C3 fragments having erythro configuration between C2 and C3. Rotamers about C1–C2 bonds are designated **gg**, **gt**, and **tg**, while rotamers about C2–C3 are designated **A**, **B**, and **C**. Rotamers **A** and **B** are associated with small vicinal coupling constants between H2 and H3, while rotamer **C** gives rise to larger values of $J_{2,3}$. Equilibria have been indicated between important conformations.

**Anthroate/C3-Cinnamate Interactions Contributing to CD: 2,3-Erythro.** It has been generally observed[1,22] that 1,3 interactions give rise to larger CD couplets than 1,2 interactions. This is due

(19) Harada, N.; Chen, S.-M. L.; Nakanishi, K. *J. Am. Chem. Soc.* **1975**, *97*, 5345.
(20) Heyn, M. P. *J. Phys. Chem.* **1975**, *79*, 2424–2426.

(21) (*R,S*) configurational assignments can vary with alkyl substituent: note that while the 1,2-diol derivative **9** is designated *S*, all of the other 31 triols, tetrols, and pentols have the same absolute stereochemistry at C2 as **9** and yet are designated 2*R*.
(22) Harada, N.; Saito, A.; Aoki, K.; Uda, H.; Sato, H. *Proceedings of the F.E.C.S. Second International Conference on Circular Dichroism*; Katjár, M., Ed.; Budapest, 1987; pp 209–214.

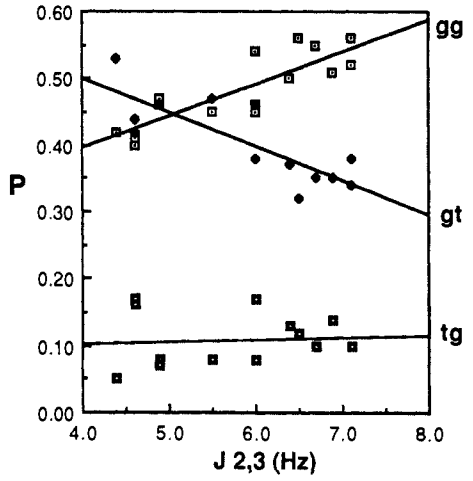


**Figure 7.** Graphical analysis of erythro conformations. Mole fractions ($P$) of the three C1–C2 rotamers (**gg**, **gt**, and **tg**) vs $J_{2,3}$ (data from Table I).

to the possibility of shorter interchromophoric distances when the chromophores are separated by a three-carbon chain. (The same geometrical constraints on interchromophoric distances explain why 1,3-diarylalkanes form intramolecular excimers better than the corresponding 1,2 compounds.[23]) Thus, we can expect the interactions between anthroate chromophores at C1 and cinnamate chromophores at C3 to make important contributions to the CD spectra of our acyclic polyol derivatives.

However, determination of the relative orientations between these chromophores is less straightforward. The C1–C2 rotamers must be considered together with the three possible C2–C3 rotamers, giving rise to nine possible conformations, as shown in Figure 6 for C2–C3 erythro derivatives. Here the C2–C3 rotamers have been designated **A**, **B**, and C, while the C1–C2 rotamers are designated as above by **gg**, **gt**, and **tg**. In this way, each of the nine rotamers can be described by a combination of two descriptors, i.e. **gg/A**, **gg/B**, etc.

Extensive conformational studies of acetylated acyclic sugar derivatives by Horton and co-workers[24] contributed to the understanding that the avoidance of 1,3-parallel interactions between syn periplanar substituents, particularly oxygen atoms, is the most important determinant of conformation in acyclic molecules. Examination of the nine possible erythro conformations reveals that four contain this type of sterically unfavorable interaction: **gg/A** and **tg/B** have 1,3-parallel interactions between O1 and the alkyl group R, while **gg/B** and **tg/C** have 1,3-parallel interactions between O1 and O3. Thus, we can expect negligible proportions of these four conformations.

While it has been possible to calculate the distribution of C1–C2 rotamers, determining the distribution of C2–C3 rotamers is more difficult. Rotamer C is characterized by a large $J_{2,3}$ value, yet both **A** and **B** are associated with small values. Thus, $J_{2,3}$ only provides an indication of $P_C$ vs ($P_A$ + $P_B$). However, CD also provides conformation information. We have previously shown that **A** and **B** rotamers give rise to equal yet opposite CD couplets centered around 311 nm due to cinnamate/cinnamate coupling. The observation that erythro derivatives display either no net effect or in certain cases a net positive couplet in this region indicates that **A** < **B**.[1] Finally, though we may know that both **gt** and C, for example, are major rotamers about each of the two bonds, there may be no indication that these two rotamers occur *simultaneously* to give rise to the **gg**/C conformation.

(23) See for example: (a) De Schryver, F. C.; Collart, P.; Vandendriessche, J.; Goedeweeck, R.; Swinnen, A.; Van der Auweraer, M. *Acc. Chem. Res.* **1987**, *20*, 159–166. (b) Becker, H.-D. *Pure Appl. Chem.* **1982**, *54*, 1589–1604. (c) Hirayama, F. *J. Phys. Chem.* **1965**, *42*, 3163–3171.
(24) (a) Blanc-Muesser, M.; Defaye, J.; Horton, D. *Carbohydr. Res.* **1980**, *87*, 71–86. (b) Horton, D. *Pure Appl. Chem.* **1975**, *42*, 301–325. (c) Defaye, J.; Gagnaire, D.; Horton, D.; Muesser, M. *Carbohydr. Res.* **1972**, *21*, 407–416. (d) Horton, D.; Wander, J. D. *Carbohydr. Res.* **1969**, *10*, 279–288.

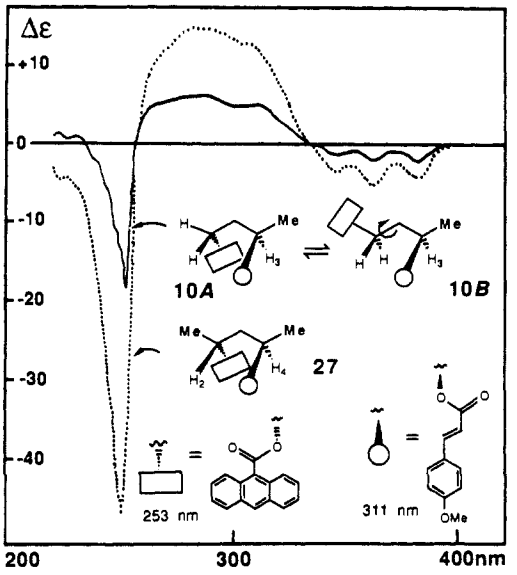


**Figure 8.** CD spectra of (*R*)-1,3-butanediol 1-(9-anthroate) 3-*p*-methoxycinnamate (**10**) and its expected conformations (***A*** and ***B***) and an analogous derivative **27** prepared from (2*R*,4*R*)-2,4-pentanediol. In **27**, the extended conformation corresponding to **10A** predominates, giving rise to a similar though more intense CD spectrum in **27** as compared with **10**. The comparison demonstrates that conformation ***A*** is largely responsible for the spectrum of **10** and serves as a model for the anthroate/C3-cinnamate coupling that occurs in erythro derivatives.

To better understand the distribution of conformations resulting from rotations about both the C1–C2 and C2–C3 bonds, we have examined the possible relationships between them. Namely, we have graphically analyzed the interdependence of the C1–C2 rotameric distributions and the $J_{2,3}$ coupling constant, as shown in Figure 7. First, the **gg** rotamer can be seen to show a strong preference for larger values of $J_{2,3}$, which, as shown in Figure 6, are associated with the C rotamer. This is undoubtedly due to the avoidance of **gg/A** and **gg/B**, both of which have sterically unfavorable 1,3-parallel interactions as discussed above. Thus, in erythro derivatives, only the **gg**/C conformation accommodates the major **gg** rotamer and must therefore be a dominant conformation.

Likewise, the **gt** rotamer shows a strong preference for smaller values of $J_{2,3}$ (Figure 7), indicating that **gt/A** and **gt/B** combined are preferred over **gt**/C. This either reflects the preference for gauche orientations between O2 and O3 (**gt/A** and **gt/B**) over the anti orientation (**gt**/C) or is simply due to the degeneracy offered by **gt/A** and **gt/B**. In any case, all of these **gt** conformations are expected to be represented. Finally, the minor **tg** rotamer shows no dependence upon $J_{2,3}$, probably because only one conformation, **tg/A**, can accommodate it without incurring an unfavorable 1,3-parallel interaction. Thus, in addition to the predominant **gg**/C conformation that is expected to account for 40–50%, the erythro derivatives assume four minor conformations as well. Three of these have the **gt** orientation about the C1–C2 bond (accounting for a total of 35–45%), and one, **tg/A**, is expected to account for 5–15% of the distribution.

CPK modeling of the major **gg**/C conformation suggests a negative chirality between the anthroate long axis C3-cinnamate transitions:

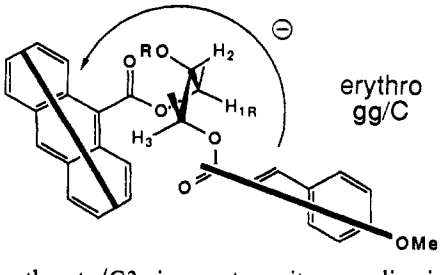


Thus, the anthroate/C3-cinnamate exciton coupling in this con-

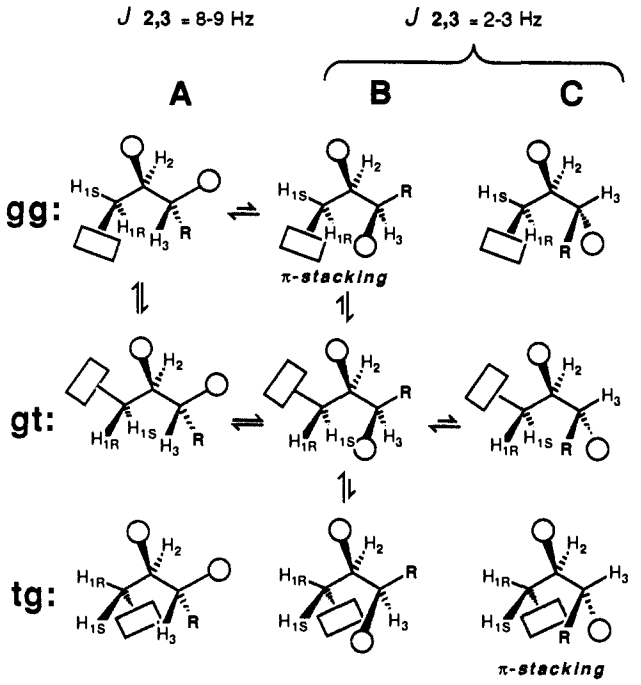


**Figure 9.** The nine possible conformations of C1–C3 fragments having threo configuration between C2 and C3. Rotamers **B** and **C** are associated with small vicinal coupling constants between H2–H3, while rotamer **A** gives rise to larger values of $J_{2,3}$. Stacking conformations (**gg/B** and **tg/C**), which may be responsible for upfield shifts of the type shown in Figure 1, have been indicated, as have equilibria between important conformations.

formation would be expected to contribute to a negative first CE at 311 nm and a positive second CE at 253 nm in the CD spectra of erythro derivatives. Superimposition of this effect upon the contributions from anthroate/C2-cinnamate coupling described above should increase the $\Delta\epsilon$ of the positive 253-nm CE. Indeed, the derivatives with D-erythro stereochemistry are characterized by very strong, positive, 253-nm CEs, as indicated in Table I.

CD curves resulting from this type of anthroate/C3-cinnamate interaction are shown in Figure 8 for two simple model compounds. (Note, however, that the stereochemistry at C3 in these compounds is opposite to that in the D-erythro derivatives above.) The first example, (*R*)-1,3-butanediol 1-(9-anthroate) 3-*p*-methoxycinnamate (**10**),[6] is expected to adopt two conformations (A and B), both of which have an extended carbon chain. Conformation ***A*** corresponds to **gg/C**, while conformation ***B*** has the anthroate in the extended position analogous to the **gt** conformations. Models indicate that the interchromophoric distance in ***B*** is larger than that in ***A***, suggesting that conformation ***A*** makes the more important contribution to the CD of **10**. This is illustrated by the CD curve of an analogous derivative **27** prepared from (2*R*,4*R*)-2,4-pentanediol (Figure 8). NMR indicates that this derivative adopts the expected conformation with an extended carbon chain, which, as shown in Figure 8, has the same orientation of chromophores as in **10*A***. The similar shape yet greater amplitude seen in the CD spectrum of **27** indicates that it is the coupling in conformation ***A*** which is responsible for the spectrum of **10**. Likewise, the anthroate/C3-cinnamate coupling in the **gg/C** conformation accounts for the stronger 253-nm CE in erythro derivatives. The minor conformations adopted by erythro derivatives are expected to give rise to negligible anthroate/C3-cinnamate couplings (i.e. **gt/A**), or small couplings with opposing chiralities (**gt/B** vs **gt/C**, Figure 6).

**Conformations in 2,3-Threo Derivatives: Aromatic Ring Stacking.** The nine possible conformations about the C1–C3 fragment of 2,3-threo derivatives are shown in Figure 9. In two of these conformations, namely **gg/B** and **tg/C**, energetically unfavorable 1,3-parallel interactions occur between the anthroate and C3-cinnamate acyloxy substituents. However, contrary to the erythro series analyzed above, NMR chemical shifts provide evidence for the existence of one or both of these conformations in the series of threo derivatives. The chemical shift of a single vinylic cinnamate proton has been found to depend upon the relative configuration between C2 and C3. In derivatives with threo configuration, this proton, $H_\alpha$, is always shifted upfield from the same proton in the corresponding erythro derivatives (see Tables I and II). This effect can be seen in the NMR spectrum shown in Figure 1, in which one of the four vinylic protons is shifted to 6.0 ppm from the typical 6.3–6.4-ppm range.

Upfield shifts have been found to be characteristic of aromatic ring stacking in many varied systems, including host–guest complexation,[25-28] amino acid/nucleotide interactions,[29] intercalation,[30] and intramolecular ligand–ligand interactions in certain metal ion complexes.[31,32] Aromatic groups separated by a three-carbon chain have the greatest propensity to adopt an intramolecular "sandwich" conformation in which the aromatic rings are stacked.[23] Intramolecular $\pi$–$\pi$-stacking between the anthroate C3-cinnamate groups, such as in **gg/B**, can account for the upfield shifts of the $H_\alpha$ proton:

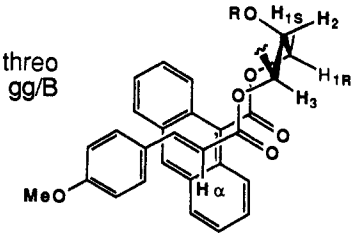


Here this proton of the C3-cinnamate is positioned directly over the anthroate ring. Strongly shielding ring current effects would result in an upfield shift of $H_\alpha$. Comparison of anthroate cinnamate derivatives **27** and **28** suggests that the upfield is indeed associated with a syn orientation between the two chromophores:

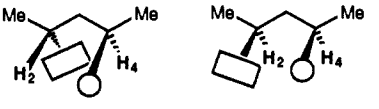

**27** Hα 6.30 ppm **28** Hα 6.22 ppm

The assignment of the upfield shifted $H_\alpha$ proton to the cinnamate group at C3 was confirmed by comparison to simple symmetric model compounds **29** and **30** in which only two types of cinnamate groups are present:

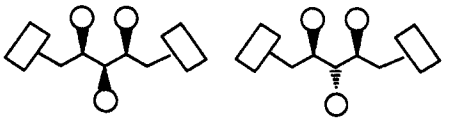

**29** (threo/threo) 6.36 ppm (2H) 5.95 ppm (1H) **vs.** **30** (erythro/erythro) 6.38 ppm (2H) 6.30 ppm (1H)

(25) (a) Colquhuon, H. M.; Stoddart, J. F.; Williams, D. J.; Wolstenholme, J. B.; Zarzycki, R. *Angew. Chem., Int. Ed. Engl.* **1981**, *20*, 1051–1053. (b) Colquhuon, H. M.; Goodings, E. P.; Maud, J. M.; Stoddart, J. F.; Williams, D. J.; Wolstenholme, J. B. *J. Chem. Soc., Chem. Commun.* **1983**, 1140–1142.
(26) (a) Rebek, J., Jr. *Science (Washington, DC)* **1987**, *235*, 1478–1484. (b) Rebek, J., Jr.; Askew, B.; Ballester, P.; Buhr, C.; Jones, S.; Nemeth, D.; Williams, K. *J. Am. Chem. Soc.* **1987**, *109*, 5033–5035. (c) Jeong, K. S.; Rebek, J., Jr. *J. Am. Chem. Soc.* **1988**, *110*, 3327–3328.
(27) (a) Hamilton, A. D.; Van Engen, D. *J. Am. Chem. Soc.* **1987**, *109*, 5035–5036. (b) Goswami, S.; Hamilton, A. D.; Van Engen, D. *J. Am. Chem. Soc.* **1989**, *111*, 3425–3426.
(28) Echavarren, A.; Galán, A.; Lehn, J.-M.; de Mendoza, J. *J. Am. Chem. Soc.* **1989**, *111*, 4994–4995.
(29) (a) Kamiichi, K.; Doi, M.; Nabae, M.; Ishida, T.; Inoue, M. *J. Chem. Soc., Perkin Trans. II* **1987**, 1739–1745. (b) Ishida, T.; Ohnishi, K.; Doi, M.; Inoue, M. *Chem. Pharm. Bull.* **1989**, *37*, 1–4.
(30) Patel, D. *Acc. Chem. Res.* **1979**, *12*, 118.
(31) (a) Sigel, H.; Malini-Balakrishnan, R.; Häring, U. K. *J. Am. Chem. Soc.* **1985**, *107*, 5137–5148. (b) Malini-Balakrishnan, R.; Scheller, K. H.; Häring, U. K.; Tribolet, R.; Sigel, H. *Inorg. Chem.* **1985**, *24*, 2067–2076.
(32) (a) Yamauchi, O.; Odani, A. *J. Am. Chem. Soc.* **1985**, *107*, 5938–5945. (b) Odani, A.; Deguchi, S.; Yamauchi, O. *Inorg. Chem.* **1986**, *25*, 62–69.

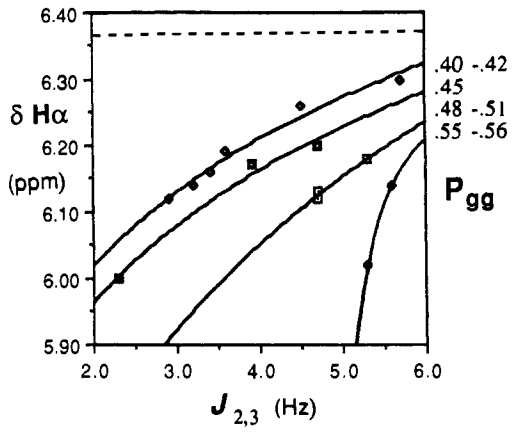


**Figure 10.** Dependence of $H_\alpha$ chemical shift in threo derivatives upon both $J_{2,3}$ and $P_{gg}$ (data from Table II). Data have been divided into four groups based upon the mole fraction of the **gg** C1–C2 rotamer. Logarithmically fit curves approach the limit of ~6.36 ppm, the chemical shift of $H_\alpha$ in the absence of aromatic stacking effects.

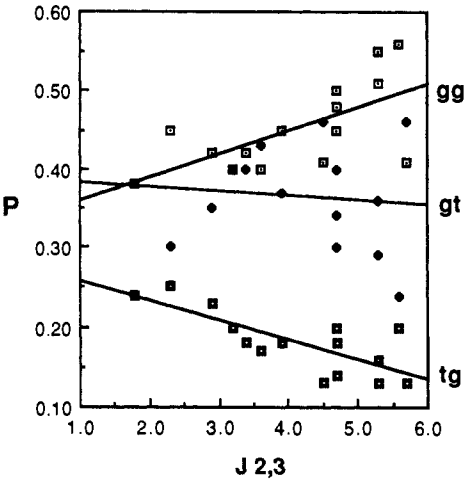


**Figure 11.** Graphical analysis of threo conformations. Mole fractions (*P*) of the three C1–C2 rotamers (**gg**, **gt**, and **tg**) vs $J_{2,3}$ (data from Table II).

The $H_\alpha$ proton of the central C3-cinnamate group in the xylitol derivative **29** (threo/threo configuration) is distinguished by integration. In this case, the upfield shift is even greater than observed in the above threo derivatives (Table II) because of the possibility of stacking with either anthroate group. The ribitol derivative **30** (erythro/erythro configuration) serves as a control, confirming that the dramatic upfield shifts are indeed associated with the threo configuration. When the NMR spectra are recorded in benzene instead of acetonitrile, no appreciable differences chemical shift differences are observed between **29** and **30**. This indicates that the upfield shifts are indeed a result of intramolecular aromatic ring stacking, as benzene is known to disrupt stacking conformations.

Xylitol derivatives such as **29** are known to adopt two bent "sickle" conformations.[1,24] Only the **gg/B** orientation offers the possibility of aromatic ring stacking between an anthroate and the central C3-cinnamate group in each of these enantiomeric conformations:

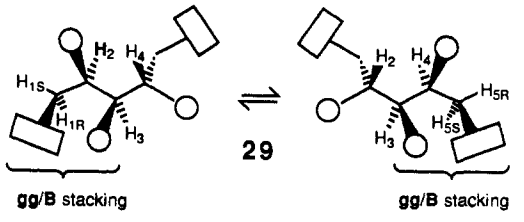


We can conclude that the observed upfield shifts result from stacking in the **gg/B** conformation rather than in the **tg/C** conformation. The latter can be expected to be less favored owing to the anti orientations between both O1/O2 and O2/O3 pairs. Note that the **tg/C** conformation in erythro derivatives (Figure 6) has a similar orientation of acyloxy substituents as well as an extended alkyl chain, and yet upfield shifts are not observed in the erythro series.

The dependence of the upfield shift upon both the **gg** rotamer and the $J_{2,3}$ values is shown in Figure 10 in which the threo data from Table II are divided into four different groups on the basis of calculated **gg** mole fractions. The curves show that for constant values of $P_{gg}$, the upfield shifting (and thus the aromatic stacking) increases with decreasing $J_{2,3}$ values. More importantly, the set of curves indicate that for constant $J_{2,3}$ values, the extent of aromatic stacking increases with increasing proportions of the **gg** rotamer. Conversely, with increasing $J_{2,3}$ values and smaller fractions of **gg**, the curves approach a limit of ~6.35 ppm, the chemical shift of the isolated $H_\alpha$ proton in the absence of stacking effects. The relationships illustrated in Figure 10 serve to confirm the conclusion that it is the **gg/B** conformation that is responsible for the observed upfield shifts.

Having positively confirmed the existence of **gg/B**, an unexpected conformation stabilized by aromatic ring stacking, the distribution of 2,3-threo conformations (Figure 9) has been analyzed by applying the same type of graphical procedures used above for the 2,3-erythro derivatives. The interdependence of the C1–C2 rotameric distributions and the $J_{2,3}$ coupling constant is shown in Figure 11. The proportion of the predominant **gg** rotamer increases with increasing values of $J_{2,3}$ coupling constants. This reflects the greater stability of **gg/A** (Figure 9) in comparison to **gg/B**, which has the 1,3-parallel interaction discussed above, and **gg/C**, which has an unfavorable 1,3-parallel interaction between aryloxy and alkyl substituents. Lacking both the favorable gauche orientation of O2–O3 and the aromatic stacking interaction which offer stabilization to **gg/B**, the **gg/C** conformation is not likely to be important. The combined mole fraction of **gg/A** and **gg/B** is on the order of 40–50%, with **gg/B** accounting for only a minor fraction of this total.

The **gt** rotamer shows little dependence upon $J_{2,3}$ (Figure 11), and this is due to the lack of any steric interaction involving the extended anthroate group. Again, as in the erythro derivatives analyzed above, each of the three possible **gt** conformations depicted in Figure 9 is probably represented, with the proportion of **gt/C** expected to be the least. Together these three would account for ~30–40% of the total, their balance depending upon the configuration of any additional centers. For example, our previous conformational analysis indicated that the C2–C3 rotamer **B** predominates in derivatives with lyxo configuration at the first three asymmetric centers (**16**, **23**, and **24**, Table II).[1]

Finally, the **tg** rotamer shows a clear preference for smaller $J_{2,3}$ values (Figure 11). This reflects the unfavorability of **tg/A** (associated with a large $J_{2,3}$ value) in which the anthroate and alkyl groups would be in a 1,3-parallel orientation. Since the **tg/C** conformation may be considered negligible for the reasons discussed above, the **tg/B** conformation is expected to account for all of the 15–25% calculated for **tg**.

**Anthroate/C3-Cinnamate Interactions Contributing to CD: 2,3-Threo.** The D-threo polyol derivatives are characterized by 253-nm Cotton effects that are smaller than the corresponding D-erythro derivatives (compare $\Delta\epsilon$'s, Tables I and II). The range of $\Delta\epsilon$'s (+24 to −7) is smaller than that of the corresponding diol derivative **9**, which contains only a single asymmetric center. Thus, we can expect that the anthroate/C3-cinnamate interaction in threo derivatives gives rise to this reduction of the positive 253-nm CE. A positive chirality between anthroate and C3-cinnamate transitions would give rise to a negative 253-nm CE and account for the net reduction of the positive CE caused by anthroate/C2-cinnamate coupling.

To determine which conformations are responsible for negative contributions at 253 nm, the CD data can be analyzed graphically to determine its dependence upon conformation. A plot of $J_{2,3}$ values versus the 253-nm $\Delta\epsilon$ data from Table II is shown in Figure 12a. Negative contributions to this Cotton effect are shown to

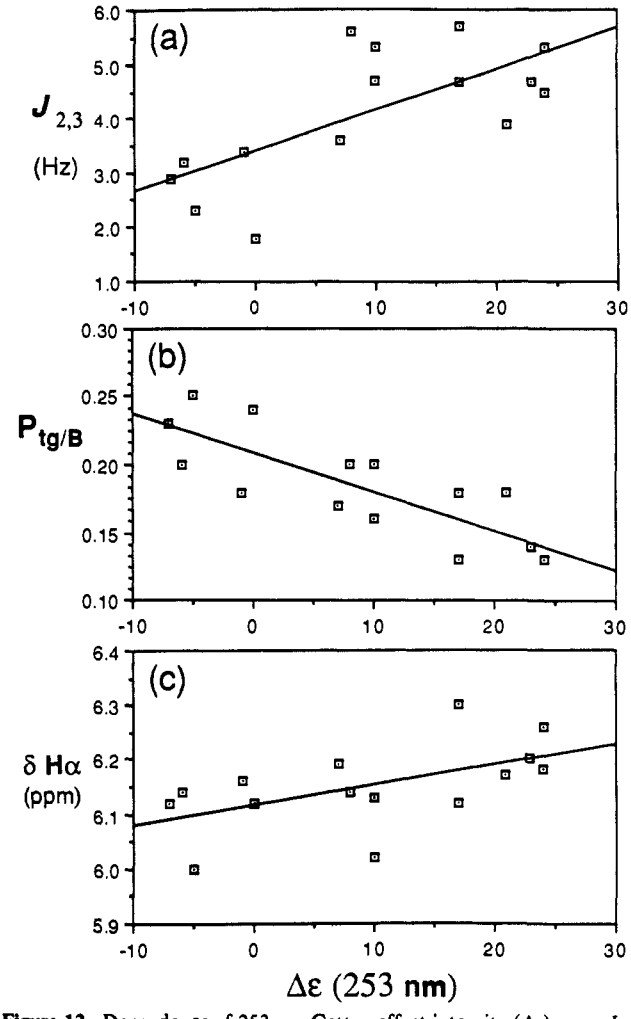


**Figure 12.** Dependence of 253-nm Cotton effect intensity ($\Delta\epsilon$) upon $J_{2,3}$, $P_{tg/B}$, and $H_\alpha$ chemical shift in threo derivatives (data from Table II). (a) Negative contributions to $\Delta\epsilon$ are shown to be associated with smaller $J_{2,3}$ values, corresponding to C2–C3 rotamer **B**. (b) Mole fraction of **tg/B** conformation shown to be directly related to smaller and more negative $\Delta\epsilon$'s. (c) Smaller and more negative $\Delta\epsilon$'s associated with decreasing $H_\alpha$ chemical shifts, corresponding to increasing proportions of the **gg/B** conformation.

be dependent upon decreasing $J_{2,3}$ values, indicating that **gg/B** and/or **tg/B** are responsible for this effect. These two threo conformations were found to be important in the analysis above and have relatively short interchromophoric distances between the anthroate and cinnamate groups. Greater interchromophoric distances in other conformations significantly reduce their relative potential to make important contributions to the CD spectra.

From the above conformational analysis it was concluded that $P_{tg/B}$ was roughly equal to $P_{tg}$ because other **tg** conformations were negligible. A plot of $P_{tg/B}$ vs $\Delta\epsilon$ (253 nm) indicates that this conformation is associated with a negative contribution to this Cotton effect (Figure 12b). The anthroate/C3-cinnamate interaction in this conformation is exactly the same as the interaction in compound **27**, the CD of which is shown above in Figure 8:

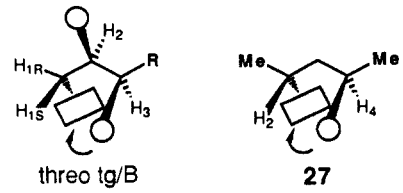


threo tg/B **27**

In **27** the extended conformation shown above predominates, and this gives rise to a $\Delta\epsilon$ of −46 at 253 nm (Figure 8). If the **tg/B** conformation shown for threo derivatives exists in only 15–25%, then we would expect the net contribution of anthroate/C3-cinnamate coupling from this conformation to be approximately a $\Delta\epsilon$ of −10 at 253 nm, or roughly one-fifth of the total observed for **27**. While this conformation clearly contributes to the reduction of the 253-nm CE, which has been found to be characteristic in the D-threo series, it cannot fully account for the ~30 $\Delta\epsilon$ reductions that in certain cases result in a negative 253-nm CE.

The intensity of CD spectra in a variety of systems has been shown to depend upon the extent of intramolecular[33] and intermolecular[34] aromatic ring stacking interactions. Thus, the stacking **gg/B** conformation may also make an important contribution to the 253-nm Cotton effect. A plot of $H_\alpha$ chemical shift vs 253-nm $\Delta\epsilon$'s indicates that the upfield shifting of this proton which occurs in the **gg/B** conformation is also associated with a negative contribution at 253 nm (Figure 12c). The extreme proximity of the two stacked chromophores in this conformation would be expected to strongly affect the CD spectrum. CPK models of this conformation indicate a positive chirality between the C3-cinnamate and the long axis transition of the anthroate chromophore:

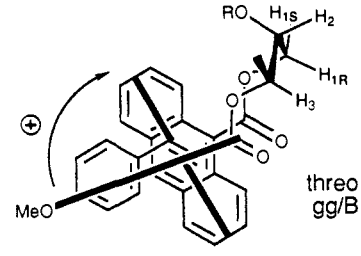


Thus, this conformation is also expected to make a negative contribution at 253 nm, in addition to a positive first CE at 311 nm. Though this conformation may account for only a small percentage of total conformations, it would have a strong effect upon the CD of threo derivatives. With the two chromophores stacked together, the interchromophoric distance is the shortest attainable (~3.5 Å). Additionally, the dihedral angle between the two coupled transitions is very near the theoretically optimal angle (70°).[19] The exceedingly strong exciton coupling that would occur in this minor conformation undoubtedly makes an important contribution to the characteristically smaller and sometimes even negative 253-nm CEs in the CD spectra of polyol derivatives with 2,3-threo configuration.

## Conclusion

The ability to rationally assign CD spectra resulting from exciton coupling illustrates the straightforward, nonempirical basis of the exciton chirality method. The CD curves of derivatives containing three or more chromophores reflect the additive effects of pairwise interactions.[4a] CD is highly sensitive to conformational differences because individual conformations can contribute widely different effects to the overall spectrum. When more than one conformation exists, the resulting CD spectrum represents a weighted average of the spectra that would result from each individual conformation.

We have developed a technique for assigning stereochemistry in acyclic polyols that utilizes two different types of exciton chromophores, and the resulting "fingerprint" CD curves can be used to make empirical assignments of up to four asymmetric centers in a single measurement. The factors giving rise to the characteristic spectra have now been fully elucidated for the various possible configurations and shown to be in complete accord with the principles of exciton coupling. Thus, this CD technique can be confidently applied to acyclic polyols with 1,2,3, 1,2,3,4, or a variety of other hydroxylation patterns. This method can

(33) (a) Miles, D. W.; Urry, D. W. *J. Phys. Chem.* **1967**, *71*, 4448–4454. (b) Miles, D. W.; Urry, D. W. *J. Biol. Chem.* **1968**, *243*, 4181–4188. (c) Miles, D. W.; Urry, D. W. *Biochemistry* **1968**, *7*, 2791–2799. (d) Ikehara, M.; Uesugi, S.; Yasumoto, M. *J. Am. Chem. Soc.* **1970**, *92*, 4735–4736.
(34) Hoshino, T.; Matsumoto, U.; Harada, N.; Goto, T. *Tetrahedron Lett.* **1981**, *22*, 3621–3624.

certainly be extended to any number of acyclic molecules that have derivatizable functional groups at chiral centers by empirical comparisons of unknowns to simple synthetic models. We have shown, however, that exciton-split CD spectra are governed by a few straightforward principles. Analysis and interpretation is possible whenever the mutual orientation between chromophores can be determined. The detailed interpretations that have been presented in these two papers[1] have elucidated a number of exciton interactions associated with various conformations and configurations that can serve as models in future studies of this type.

Our approach to the conformational analysis of acyclic sugar derivatives benefited from having a large number of configurationally related examples. A process of graphic analysis to determine interdependencies between coupling constants or other conformationally dependent data was introduced. By this approach, we were able to demonstrate the existence of a minor conformation having a 1,3-parallel interaction between oxygen atoms, contradicting earlier generalizations that excluded such a conformation from consideration. Recent reports have demonstrated that 1,3-parallel interactions between oxygen atoms can be stabilized by hydrogen bonds between hydroxyl groups.[35,36] Studies presented here indicate that $\pi-\pi$ stacking interactions can also offer some degree of stabilization to conformations with 1,3-parallel interactions between oxygen atoms. The dependence of exciton coupling upon interchromophoric distance makes consideration of these previously unexpected conformations particularly important for CD spectral analysis.

## Experimental Section

$^1$H NMR spectra were recorded on a Brucker WM250 operated at 250 MHz. Conformational analysis by NMR was carried out in $CD_3CN$ in order to corroborate findings with CD spectra. Vicinal coupling constants were determined by first-order analysis. Other NMR spectra were recorded in $CDCl_3$ or $CD_3OD$. UV measurements (acetonitrile) were performed on a Perkin-Elmer 320 UV spectrophotometer. CD spectra (acetonitrile) were recorded from 420-220 nm on a JASCO 500A spectropolarimeter driven by a JASCO DP500N data processor (1-cm quartz cell; ambient temperature; sensitivity 2 mdeg/cm; all spectra normalized to 10 $\mu$M for comparison purposes).

Prior to UV and CD measurements, all samples were purified by HPLC (EtOAc-hexane 3:7; 5 $\mu$m YMC $SiO_2$ gel; 2 mL/min; 311 nm UV detection). UV measurements were performed on 5-15 $\mu$M acetonitrile solutions, the concentrations of which were determined on the basis of the approximate extinction coefficient: anthroate monocinnamates $\epsilon_{311nm} = 28\,400$.

**General Procedure.** The sugar derivatives were treated with 1.1 equiv of 9-anthroyl chloride in dry pyridine (1-2 mL) with a small amount of DMAP (acylation catalyst).[37] After being stirred overnight under $N_2$, the reaction mixtures were frozen (to prevent bumping), and pyridine was removed in vacuo (1 mmHg) upon warming. Crude reaction mixtures was purified directly without workup by flash chromatography[38] ($MeOH/CH_2Cl_2$ mixtures). Subsequent treatment with excess *p*-methoxycinnamoyl chloride in a similar manner afforded the mixed anthroate cinnamate esters.

**(6*S*)-(6-$^2H_1$)-1-Deoxy-D-galactitol (5).** (6*S*)-(6-$^2H_1$)-D-Galactose[7a] (**4**, 100 mg) was refluxed in anhydrous hydrazine (4 mL) under argon for 48 h as previously reported for undeuterated D-galactose.[1] The reaction mixture was then frozen under argon and the hydrazine was removed under high vacuum. NMR of the crude residue indicated a mixture of desired pentitol (50%) together with 1,2-dideoxyhexitol and hex-1-enitol products. Flash chromatography ($MeOH/CH_2Cl_2$ 3:17) afforded pure **5** (32 mg, 35%). This was derivatized to **1** by general procedures as previously reported for undeuterated galactitol.[1] $^1$H NMR ($CD_3OD$) (**5**): $\delta$ 4.05 (dq, 2.0, 6.6 Hz, 1 H, H-2), 3.89 (dd, 1.7, 6.2 Hz, 1 H, H-5), 3.64 (d, 6.2 Hz, 1 H, H-6R), 3.63 (dd, 1.7, 8.8 Hz, 1 H, H-4), 3.43 (dd, 2.0, 8.8 Hz, 1 H, H-3), 1.23 (d, 6.6 Hz, 3 H, Me).

**(6*S*)-(6-$^2H_1$)-1-Deoxy-D-glucitol (7).** (6*S*)-(6-$^2H_1$)-D-Glucose[7b] (**6**) was subjected to hydrazynolysis and hydrogenation conditions as previously described, after which a portion of the mixture was purified by flash chromatography ($MeOH/CH_2Cl_2$: gradient from 12:88 to 15:85) to give **7**. This was derivatized to **2** by general procedures as previously reported.[1] $^1$H NMR ($CD_3OD$) (**7**): $\delta$ 3.86 (dq, 1 H, H-2), 3.68 (m, 1 H, H-5), 3.61 (dd, 5.2, 10.5 Hz, 1 H, H-6R), 3.57-3.53 (m, 2 H, H-3, H-4), 1.18 (d, 6.4 Hz, 3 H, Me). By comparison to the NMR of undeuterated 1-deoxyglucitol, H-6S can be assigned to the signal at 3.78 ppm (dd, 3.0, 10.5 Hz).

**Note Added in Proof.** Prochiral aryloxymethylene protons have also been assigned in a related CD and NMR study of glycerol dibenzoates: Uzawa, H.; Nishida, Y.; Ohrui, H.; Meguro, H. *J. Org. Chem.* **1990**, *55*, 116-122.

**Acknowledgment.** These studies have been supported by NIH Grant GM 34509.

**Supplementary Material Available:** Preparations and figures showing complete spectral data for all intermediates and peracylated derivatives (14 pages). Ordering information is given on any current masthead page.

(35) Angyal, S. J.; Le Fur, R. *J. Org. Chem.* **1989**, *54*, 1927-1931.
(36) Lancelin, J.-M.; Paquet, F.; Beau, J.-M. *Tetrahedron Lett.* **1988**, *29*, 2827-2830.
(37) Hölfle, G.; Steglich, W.; Vorbrüggen, H. *Angew. Chem., Int. Ed. Engl.* **1978**, *17*, 569.
(38) Still, W. C.; Mitra, A. *J. Org. Chem.* **1978**, *41*, 2923.

# Total Synthesis of FK506 and an FKBP Probe Reagent, ($C_8$,$C_9$-$^{13}C_2$)-FK506

**Masashi Nakatsuka, John A. Ragan, Tarek Sammakia, David B. Smith, David E. Uehling, and Stuart L. Schreiber***

*Contribution from the Department of Chemistry, Harvard University, Cambridge, Massachusetts 02138.* *Received December 12, 1989*

**Abstract:** Asymmetric syntheses of FK506 and ($C_8$,$C_9$-$^{13}C_2$)-FK506 are reported. The latter compound was designed to facilitate an investigation of the interactions between FK506 and its receptor, the recently discovered immunophilin, FKBP. The syntheses involved the preparation of intermediates **7-9** in nonracemic form; the key coupling reactions included a Cram-selective addition of the vinyl Grignard reagent derived from bromide **9** to aldehyde **8** and the addition of the lithioanion of phosphonamide **7** to aldehyde **51**, followed by thermal elimination. Dithiane **65** was then hydrolyzed, and glycolic ester **6** (or **6***) was added via an aldol reaction that allowed the introduction of $^{13}C$ labels at $C_8$ and $C_9$. Elaboration to FK506 proceeded via a Mukaiyama lactamization reaction and a selective deprotection/oxidation sequence, the efficiency of which was critically dependent upon the order of protecting group removal.

The understanding of signaling processes in the T cell that lead to transcriptional regulation of the lymphokine gene locus is a central focus of current immunological research.[1] The natural products FK506 (**1**)[2] and cyclosporin A (CsA) (**3**)[3] selectively and

0002-7863/90/1512-5583$02.50/0 